The Astrophysical Journal, 604:297–305, 2004 March 20

IMPULSIVE ELECTRON ACCELERATION BY GRAVITATIONAL WAVES

Loukas Vlahos, George Voyatzis, and Demetrios Papadopoulos
Department of Physics, University of Thessaloniki, Thessaloniki 54421, Greece
Received 2003 September 8; accepted 2003 December 4

ABSTRACT

We investigate the nonlinear interaction of a strong gravitational wave with the plasma during the collapse of a massive magnetized star and subsequent formation of a black hole or during the merging of neutron star binaries (the central engine). We found that under certain conditions this coupling may result in an efficient energy-space diffusion of particles. We suggest that the atmosphere created around the central engine is filled with three-dimensional magnetic neutral sheets (magnetic nulls). We demonstrate that the passage of strong pulses of gravitational waves through the magnetic neutral sheets accelerates electrons to very high energies. Superposition of many such short-lived accelerators, embedded inside a turbulent plasma, may be the source of the observed impulsive short-lived bursts. We conclude that in several astrophysical events, gravitational pulses may accelerate the tail of the ambient plasma to very high energies and become the driver for many types of astrophysical bursts.

Subject headings: gamma rays: bursts — gravitational waves

1. INTRODUCTION

The interaction of gravitational waves (GWs) with the plasma and/or the electromagnetic waves propagating inside the plasma has been studied extensively (DeWitt & Breheme 1960; Cooperstock 1968; Zel'dovich 1974; Gerlach 1974; Grishchuk & Polnarev 1980; Denisov 1978; Macdonald & Thorne 1982; Demianski 1985; Daniel & Tajima 1997; Brodin & Marklund 1999; Marklund, Brodin, & Dunsby 2000; Brodin, Marklund, & Dunsby 2000; Brodin, Marklund, & Servin 2001; Servin et al. 2000; Servin, Brodin, & Marklund 2001; Moortgat & Kuijpers 2003). All well-known approaches to the study of the wave-plasma interaction have been used, namely, the Vlasov-Maxwell equations (Macedo & Nelson 1982), the MHD equations (Papadopoulos & Esposito 1981; Papadopoulos et al. 2001; Moortgat & Kuijpers 2003), and the nonlinear evolution of charged particles interacting with a monochromatic GW (Varvoglis & Papadopoulos 1992). The Vlasov-Maxwell equations and the MHD equations were mainly used to investigate the linear coupling of the GW with the normal modes of the ambient plasma, but the normal-mode analysis is a valid approximation only when the GW is relatively weak and the orbits of the charged particles are assumed to remain close to the undisturbed ones. Several studies have also explored, using the weak-turbulence theory, the nonlinear wave-wave interaction of plasma waves with the GW (see Brodin et al. 2000).

The strong nonlinear coupling of isolated charged particles with a coherent GW has been studied using the Hamiltonian formalism (Varvoglis & Papadopoulos 1992; Kleidis, Varvoglis, & Papadopoulos 1993; Kleidis et al. 1995). The main conclusion of these studies is that the coupling between the GW and an isolated charged particle gyrating inside a constant magnetic field can be very strong only if the GW is very intense. This type of analysis can treat the full nonlinear coupling of the charged particle with the GW but looses all the collective phenomena associated with the excitation of waves inside the plasma and the back-reaction of the plasma onto the GW.

In this article we reinvestigate the nonlinear interaction of an electron with a GW inside a magnetic field, using the Hamiltonian formalism. Our study is applicable in the neighborhood of the central engine (collapsing massive magnetic star; Fryer, Holz, & Hughes 2002; Dimmelmeier, Font, & Muller 2002; Baumgarte & Shapiro 2003) or during the final stages of the merging of neutron star binaries (Ruffert & Janka 1998; Shibata & Uryu 2002). We find that a strong but low frequency (10 KHz) GW can resonate with ambient electrons only in the neighborhood of magnetic neutral sheets and accelerates them to very high energies in milliseconds. Relativistic electrons travel along the magnetic field, escaping from the neutral sheet to the superstrong magnetic field and emitting synchrotron radiation. We propose that the passage of a GW through numerous localized neutral sheets will create spiky sources that collectively are highly variable in time.

In § 2 we analyze the interaction of a GW with a single electron inside a constant magnetic field. In § 3 we investigate the diffusion to high energies of a distribution of electrons inside the GW. In § 4 we propose a new model for strong coupling of the GW with the turbulent plasma in the atmosphere of the central engine and the resulting impulsive synchrotron emission, and finally, in § 5 we summarize our results.

2. THE HAMILTONIAN FORMULATION OF THE GW-PARTICLE INTERACTION

The motion of a charged particle in a curved space and in the presence of a magnetic field is described by a Hamiltonian, which, in a system of units $m = c = G = 1$, is given by

$$H(x^{\alpha}, p_{\alpha}) = \frac{1}{2} g^{\mu\nu}(p_{\mu} - eA_{\mu})(p_{\nu} - eA_{\nu}) = \frac{1}{2}, \quad \alpha,\ \mu,\ \nu = 0,\ \ldots,\ 3; \tag{1}$$

$g^{\mu\nu} = g^{\mu\nu}(x^{\alpha})$ are the contravariant components of the metric tensor of the curved space, and $A_{\mu} = A_{\mu}(x^{\alpha})$ are the components of the vector potential of the magnetic field (Misner, Thorne, & Wheeler 1973). The variables p_{α} are the generalized momenta corresponding to the coordinates x^{α}, and their evolution with respect to the proper time τ is given by the canonical equations

$$\frac{dx^{\alpha}}{d\tau} = \frac{\partial H}{\partial p_{\alpha}}, \quad \frac{dp_{\alpha}}{d\tau} = -\frac{\partial H}{\partial x^{\alpha}}. \tag{2}$$

We assume a constant magnetic field $\boldsymbol{B} = B_0 \boldsymbol{e}_z$, which is produced by the vector potential

$$A_0 = A_1 = A_3 = 0, \quad A_2 = B_0\left(x^1 + c_0\right), \quad c_0 = \text{const}, \tag{3}$$

and that a GW propagates in a direction $\boldsymbol{k}$ of angle θ with respect to the direction of the magnetic field. In that case the nonzero components of the metric tensor are (see Ohanian 1976; Papadopoulos & Esposito 1981) $g^{00} = 1$ and

$$g^{11} = \frac{1 - a\sin^2\theta\cos\psi}{-1 + a\cos\psi},$$
$$g^{22} = \frac{-1}{1 + a\cos\psi},$$
$$g^{33} = \frac{1 - a\cos^2\theta\cos\psi}{-1 + a\cos\psi},$$
$$g^{13} = g^{31} = \frac{(-a/2)\sin 2\theta\cos\psi}{-1 + a\cos\psi}, \tag{4}$$

where a is the amplitude of the GW and $\psi = k_\mu x^\mu = \nu(\sin\theta x^1 + \cos\theta x^3 - x^0)$. The parameter ν is the relative frequency of the GW, i.e., $\nu = \omega/\Omega$, where $\Omega = eB_0/mc$ is the Larmor angular frequency. We make use of the scaling $eB_0 = 1$, and thus $\Omega = 1$.

In the above formalism, the coordinate x^2 is ignorable, so $p_2 = \text{const}$. By setting the constant c_0 in equation (3) equal to p_2 we get an appropriate gauge that reduces by 1 degree of freedom the Hamiltonian (eq. [1]), which takes the form

$$H = \frac{1}{2}\left(p_0^2 - \frac{1 - as_\theta^2\cos\psi}{1 - a\cos\psi}p_1^2 - \frac{1 - ac_\theta^2\cos\psi}{1 - a\cos\psi}p_3^2 + \frac{2\alpha s_\theta c_\theta\cos\psi}{1 - a\cos\psi}p_1 p_3 - \frac{x_1^2}{1 + a\cos\psi}\right), \tag{5}$$

where we use the notation $c_\theta = \cos\theta$ and $s_\theta = \sin\theta$ for brevity. We apply the canonical transformation of variables $(x^0, x^1, x^3, p_0, p_1, p_3) \rightarrow (\chi, q, \phi, I, p, J)$ using the generating function

$$F\left(x^0, x^1, x^3, I, p, J\right) = x^0 I + x^1 p + \nu\left(s_\theta x^1 + c_\theta x^3 - x^0\right)J. \tag{6}$$

The relation between the old and the new variables is given by the equations

$$\chi = x^0,$$
$$q = x^1,$$
$$\phi = \nu\left(s_\theta x^1 + c_\theta x^3 - x^0\right),$$
$$I = p_0 + p_3/c_\theta,$$
$$p = p_1 - (s_\theta/c_\theta)p_3,$$
$$J = p_3/(c_\theta s_\theta). \tag{7}$$

In the new variables the Hamiltonian (eq. [5]) takes the form

$$H = \frac{1}{2}\left(I^2 - 2I\nu J - 2s_\theta\nu Jp - \frac{1 - as_\theta^2\cos\phi}{1 - a\cos\phi}p^2 - \frac{q^2}{1 + a\cos\phi}\right). \tag{8}$$

Since the variable χ is ignorable, I is a constant of motion and equation (8) can be studied as a system of 2 degrees of freedom, where I is a parameter. The variables q and p are associated with the gyromotion. H is of mod(2π) with respect to the angle variable ϕ, and the variable J is related linearly to the energy $\gamma = (1 - v^2)^{-1/2}$ of the particles according to the equation

$$\gamma = I - \nu J. \tag{9}$$

The equations of motion are

$$\dot{q} = -s_\theta\nu J - \frac{1 - as_\theta^2\cos\phi}{1 - a\cos\phi}p,$$
$$\dot{p} = \frac{q}{1 + a\cos\phi},$$
$$\dot{\phi} = -\nu I - s_\theta\nu p,$$
$$\dot{J} = \frac{a}{2}\left[\frac{q^2}{(1 + a\cos\phi)^2} - \frac{c_\theta^2 p^2}{(1 - a\cos\phi)^2}\right]\sin\phi, \tag{10}$$

where the dot means derivative with respect to the proper time τ. Furthermore, equation (8) can be written as a perturbed Hamiltonian in the usual way, i.e.,

$$H = H_0 + aH_1 + a^2 H_2 + \ldots, \tag{11}$$

where

$$H_m = -\left[c_\theta^2 p^2 + (-1)^m q^2\right]\cos^m\phi, \quad m \geq 1, \tag{12}$$

are the perturbation terms and

$$H_0 = \frac{1}{2}\left(I^2 - 2I\nu J - 2s_\theta\nu Jp\right) - \frac{1}{2}\left(p^2 + q^2\right) \tag{13}$$

is the integrable part of the system that describes the unperturbed helical motion of the particle in the flat space. Considering action-angle variables J_1, J_2, ϕ_1, and ϕ_2, equation (13) takes the form

$$H_0(J_1, J_2) = \frac{I}{2} - I\nu J_1 + \frac{s_\theta^2\nu^2}{2}J_1^2 - J_2, \tag{14}$$

where $\phi_1 = \phi$, $J_1 = J$ and

$$J_2 = \frac{1}{2\pi}\oint p\,dq = \frac{1}{2}\left(I^2 - 2I\nu J + s_\theta^2\nu^2 J^2 - 1\right),$$
$$\phi_2 = \arcsin\left(\frac{\pm q}{\sqrt{2J_2}}\right).$$

Therefore, the unperturbed system is isoenergetically nondegenerate for $\theta \neq 0$ (Arnol'd, Kozlov, & Neishtadt 1987), and the gyromotion of the particles is represented by trajectories that twist invariant tori with angular frequencies $\omega_1 = \partial H_0/\partial J_1$ and $\omega_2 = \partial H_0/\partial J_2$. The periodic or quasi-periodic evolution of the trajectories depends on whether the rotation number, defined by

$$\rho = \frac{\omega_1}{\omega_2} = \nu I - s_\theta^2\nu^2 J_1 = \nu\left(c_\theta^2 I + s_\theta^2\gamma\right), \tag{15}$$

is rational or irrational, respectively.

Most of the invariant tori will persist with the presence of the perturbation introduced by the GW if the amplitude is sufficiently small, according to the KAM theorem (Arnol'd et al. 1987). The orbits of the particles remain close to the unperturbed ones but their projection on the x^1-x^2 plane is not exactly circular and periodic. Close to the resonant tori, where ρ is rational, the Poincaré-Birkhoff theorem applies; a finite number of pairs of stable and unstable periodic trajectories survive, producing locally a pendulum-like topology in phase space (Sagdeev, Usikov, & Zaslavsky 1988).

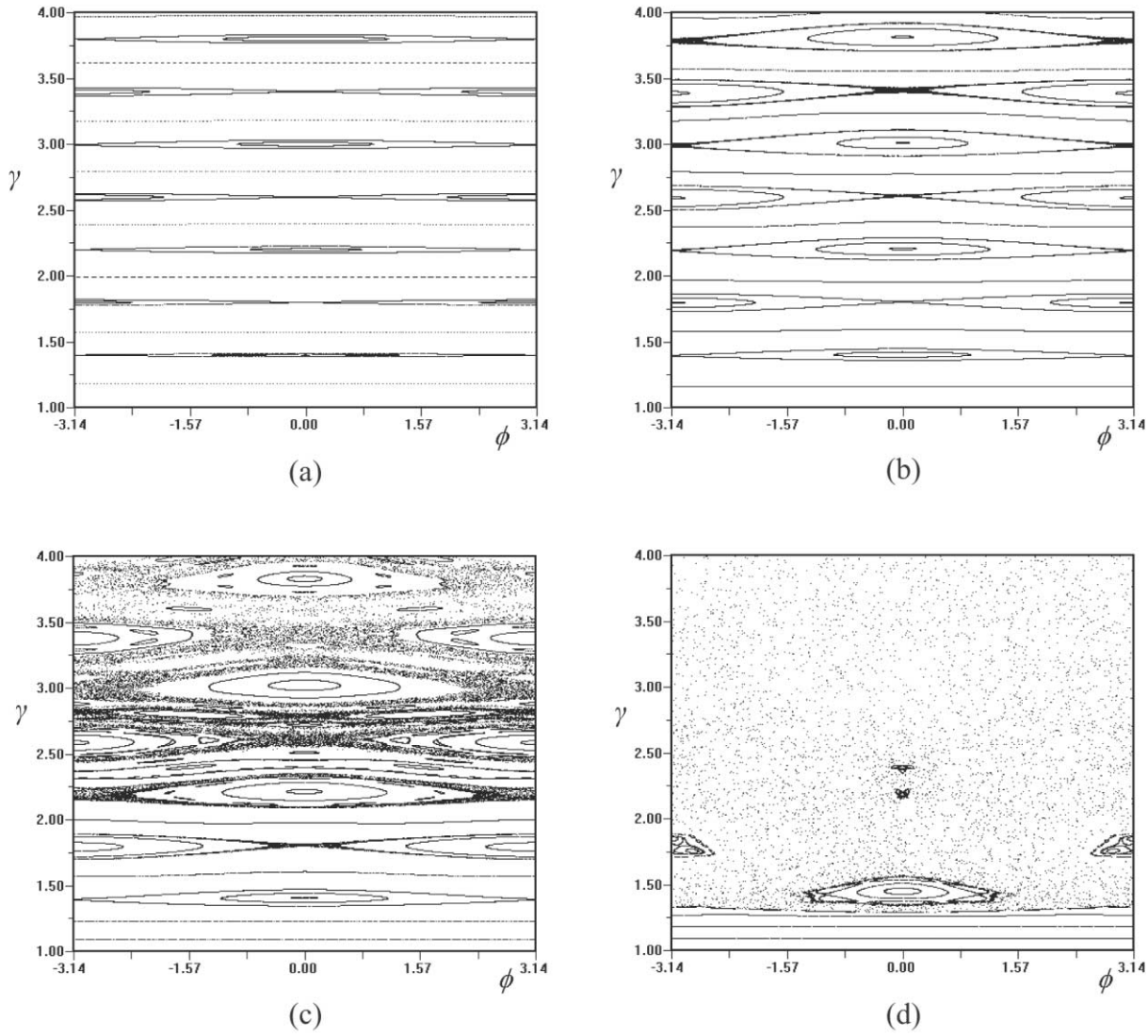

FIG. 1.—Typical Poincaré sections on the plane (ϕ, γ) of the perturbed system for $\nu = 5$, $\theta = 45^\circ$, and (*a*) $a = 0.001$, (*b*) $a = 0.01$, (*c*) $a = 0.02$, and (*d*) $a = 0.1$

Since the system is of 2 degrees of freedom, we can study its evolution by using the Poincaré sections $P_S = \{(\phi, \gamma), q = 0, H = 1/2\}$, choosing specific sets of the parameters a, I, ν, and θ. In the numerical calculations that follow, we set $I = 1$. For the unperturbed system ($a = 0$) the sections show invariant curves $\gamma = \text{const}$. For $a \neq 0$ some typical examples are shown in Figure 1.

For small values of a (Fig. 1*a*), the invariant curves are perturbed slightly, and only close to the most significant resonances does their deformation become noticeable. Increasing further the perturbation parameter a, the width of the resonances increases and homoclinic chaos becomes more obvious close to the hyperbolic fixed points (Fig. 1*b*). The existence of invariant curves, which confine the resonant regions, guarantees the bounded variation of the particle's energy $[\Delta\gamma = O(\sqrt{a})]$ for the chaotic trajectories.

When the amplitude a exceeds a critical value a_c, overlapping of resonances takes place and large chaotic regions are generated (Fig. 1*c*; see also Chirikov 1979). Particles with initial energy γ greater than a critical value γ_c may follow a chaotic orbit that diffuses to regions of higher energy, and this will lead the particles to very high energies in short timescales. For relatively large values of $\alpha_c \ll \alpha < 1$, the islands of regular motion, which survive from the resonance overlapping, are gradually destroyed and chaos extends down to relatively low energy particles (Fig. 1*d*). The chaotic part of the phase space is called "the chaotic sea."

The dynamics, presented by the Poincaré sections in Figure 1, are typical for the majority of parameter values. Generally, the critical values a_c and γ_c determine the conditions for possible chaotic diffusion. The dynamics of the charged particles show some exceptional characteristics when the frequency of the GW is comparable to the Larmor frequency of the unperturbed motion, particularly when $1 \leq \nu < 3$. For such parameter values, stochastic behavior will appear when $\gamma = 1$, and for sufficiently large perturbation values, large chaotic regions are generated and diffusion, even for particles with very low initial energies, will be possible. An example is shown in Figure 2*a*.

The evolution of the particles changes character when the direction of propagation of the GW is almost parallel to $\boldsymbol{B}$. In this case, chaos disappears and the particles undergo large energy oscillations. As shown in Figure 2*b*, a particle starting even from rest ($\gamma \approx 1$) will be driven regularly to high energies

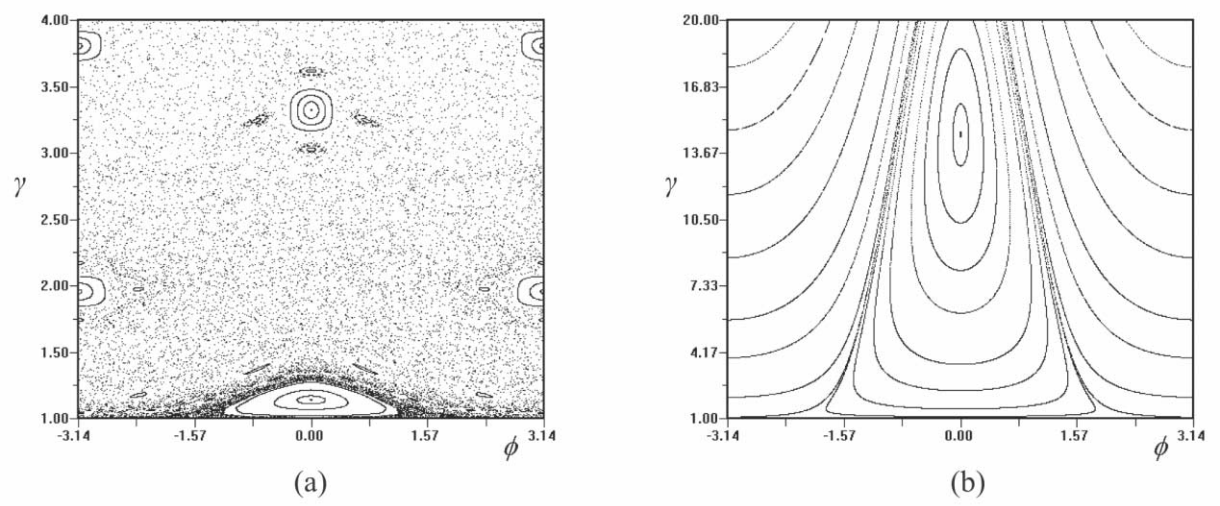

FIG. 2.—Poincaré sections on the plane (ϕ, γ) for (*a*) $a = 0.2$, $\nu = 2$, $\theta = 45^\circ$ and (*b*) $a = 0.2$, $\nu = 1$, $\theta = 5^\circ$

$(\gamma > 20)$ and returns back to its initial energy in an almost periodic way. In a realistic, non-infinite system, several particles may escape from the interaction with the GW before returning back to low energies. At $\theta = 0$ the system is integrable and the energy of the particles shows regular slow oscillations with an amplitude proportional to a.

3. CHAOTIC DIFFUSION AND PARTICLE ACCELERATION

In the previous section we showed that chaotic diffusion is possible for $a \geq a_c$ and for the particles with $\gamma \geq \gamma_c$. Such conditions are necessary but not sufficient for acceleration, since islands of regular motion may be present inside the wide chaotic region (see for example Fig. 2). We estimate approximately the critical value a_c by studying a large number of Poincaré sections for different values of θ (Fig. 3*a*). We observe that for small values of ν, resonance overlap is obtained for relatively large amplitudes of the GW. For higher frequency, $\nu > 5$, and $\theta > 45^\circ$ the overlapping of resonances takes place even for relatively small values of α. The critical value γ_c along the frequency axis ν is presented for $\theta = 45^\circ$ and for $a = 0.05$, 0.1, and 0.2 in Figure 3*b*. For large values of ν, and when the critical value a_c is relatively small ($\sim$0.005), the critical particle energy γ_c is large and increases linearly with ν. Namely, for large ν, chaotic diffusion takes place only for high-energy particles. On the other hand, for $\nu \approx 2$, resonance overlapping takes place for large perturbations but the wide chaotic sea formed extends down to the thermal velocity.

In Figure 4*a* the evolution of γ along a temporarily trapped chaotic orbit ($\gamma < \gamma_c$) and an orbit that undergoes fast diffusion is shown, using $a = 0.02$. In Figure 4*b* we plot the orbit of a particle that on average is not gaining energy and the average rate of energy gain of 200 particles. The diffusion rate of the particles in the energy space is initially fast, but for time $t > 5000$ it starts to slow down. The time t is normalized with the gyroperiod $2\pi/\Omega$

3.1. *GW Interacting with an Ensemble of Electrons*

We study next the evolution of an energy distribution $N(\gamma, t = 0)$ of electrons interacting with the GW. In Figure 5*a*

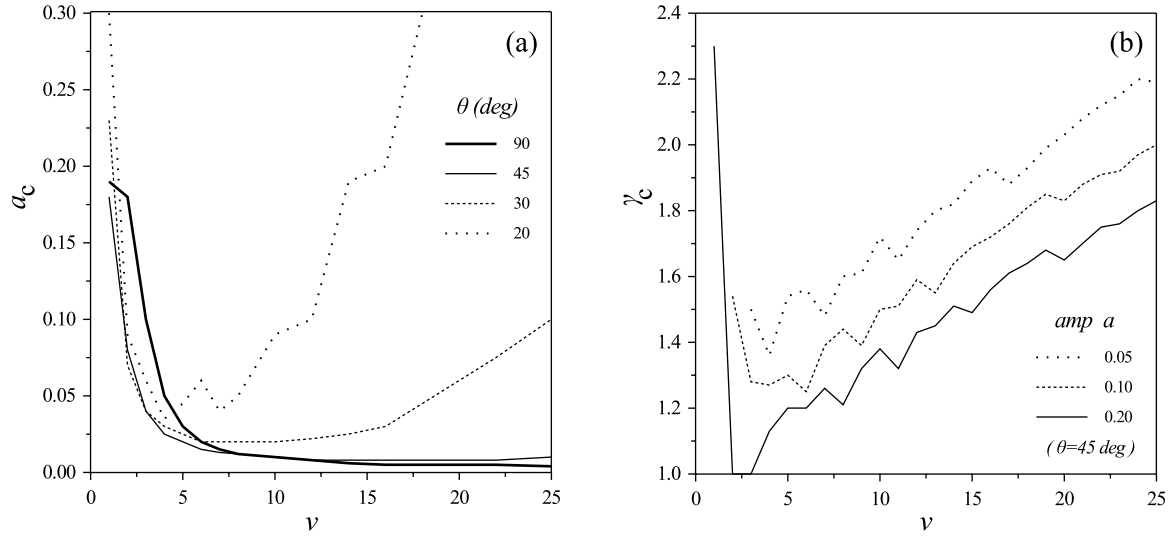

FIG. 3.—(*a*) Variation of critical value a_c with the angular frequency ν of the GW. (*b*) Same, for the critical value γ_c and $\theta = 45^\circ$, using typical values for the amplitude a.

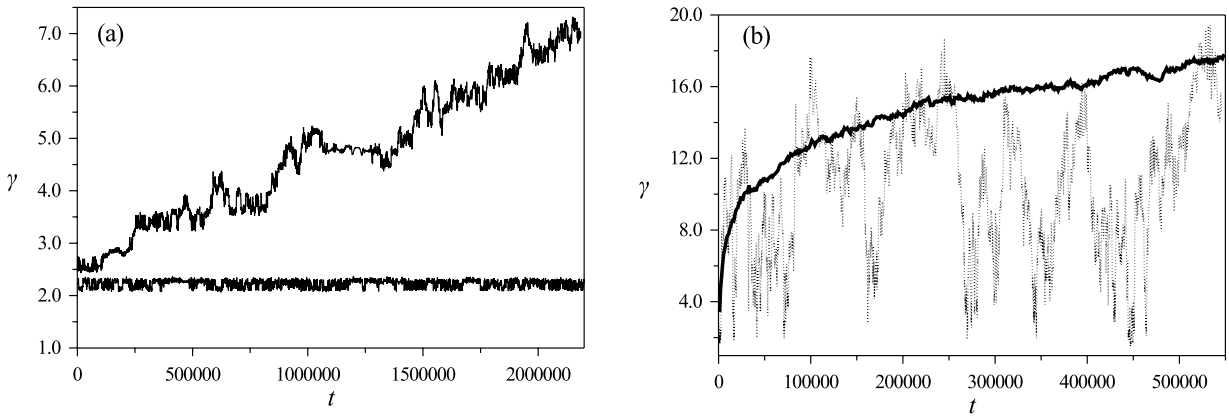

FIG. 4.—(*a*) Evolution of γ along a chaotic orbit trapped in a magnetic island for $\gamma(0) = 2.2$, $\phi(0) = \pi$ and along a diffusive one for $\gamma(0) = 2.6$, $\phi(0) = 0$ ($a = 0.02$, $\theta = 45^\circ$, $\nu = 5$). (*b*) Evolution of γ along a strongly chaotic orbit (*dotted line*) and its average value (*solid line*) along 200 trajectories starting with $\gamma(0) = 2.0$ and a randomly selected $\phi(0)$ ($a = 0.1$, $\theta = 45^\circ$, $\nu = 5$). The time is normalized with the gyroperiod $2\pi/\Omega$.

we follow the evolution of 3×10^4 particles forming initially a cold energy distribution $N(\gamma, t = 0) \sim \delta(\gamma - 3)$, where δ is the Dirac delta function; i.e., all particles have the same initial energy $\gamma = 3$. A large spread in their energy is achieved in short timescales, and for $t = 1000$, a nonthermal tail extending up to $\gamma = 100$ is formed.

We repeat the same analysis, assuming that the initial distribution is the tail ($v > V_{\rm the}$, where $V_{\rm the}$ is the ambient thermal velocity) of a Maxwellian distribution (Fig. 5*b*). The distribution of the high-energy particles forms a long nonthermal tail analogous to the results reported in Figure 5*a*.

The mean energy diffusion as a function of time is plotted in Figure 6*a* for a particular set of parameters, and it has the general form

$$\langle \gamma \rangle \sim t^d. \tag{16}$$

From a large number of calculations, we find that the energy spread in time follows a normal diffusion ($d = 0.5$) in energy space, but as α increases (see Fig. 6*b*), the interaction becomes superdiffusive ($d \geq 0.5$) in energy space. This allows electrons to spread rapidly in energy space and explains the efficient coupling between the GW and the plasma.

4. A MODEL FOR BURSTY ACCELERATION

Our main findings so far are as follows:

1. The GW can accelerate electrons from the tail of the ambient velocity distribution [$v_0(t = 0) > V_{\rm the}$] to very high energies ($\gamma > 10$–100) for typical values of $0.005 < \alpha < 0.5$ and $5 \leq \omega/\Omega \leq 20$. Assuming that the frequency of the GW is around 10 KHz and that $\Omega \sim \omega/3$, the magnetic field's strength should be around $\sim 10^{-4}$ G.
2. The acceleration time depends in general on α but is relatively short, $t_{\rm acc} \sim 100\Omega^{-1} \sim$ ms. During that time the GW will travel a distance $l_{\rm acc} \sim ct_{\rm acc} \sim 10^8$ cm.
3. The mean energy diffusion of the electrons interacting with the GW follows the simple scaling $\langle \gamma \rangle \sim t^d$.

We propose a new mechanism for efficient particle acceleration around strong and impulsive sources of GWs using the estimates presented above for the strong interaction of a GW with electrons. We assume that in the atmosphere of the

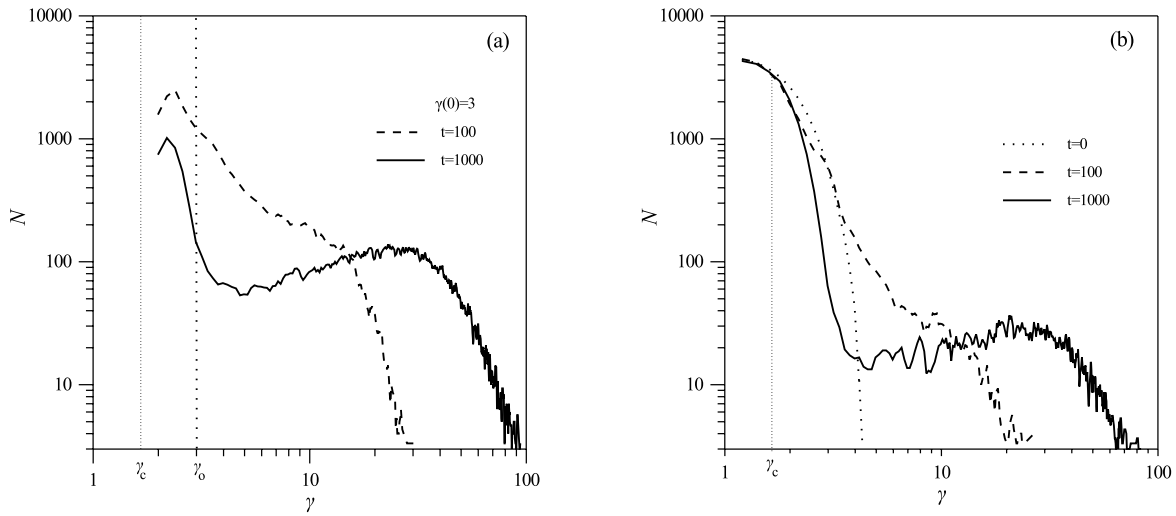

FIG. 5.—Evolution of an energy distribution. (*a*) The initial distribution (*dotted line*) consists of 3×10^4 particles having $\gamma(t = 0) = 3$. (*b*) The initial distribution is Maxwellian, as shown by the dotted curve. Only particles in the tail of the Maxwellian with $\gamma > \gamma_c$ will be accelerated. The parameters used in both studies are $a = 0.5$, $\nu = 20$, and $\theta = 30^\circ$.

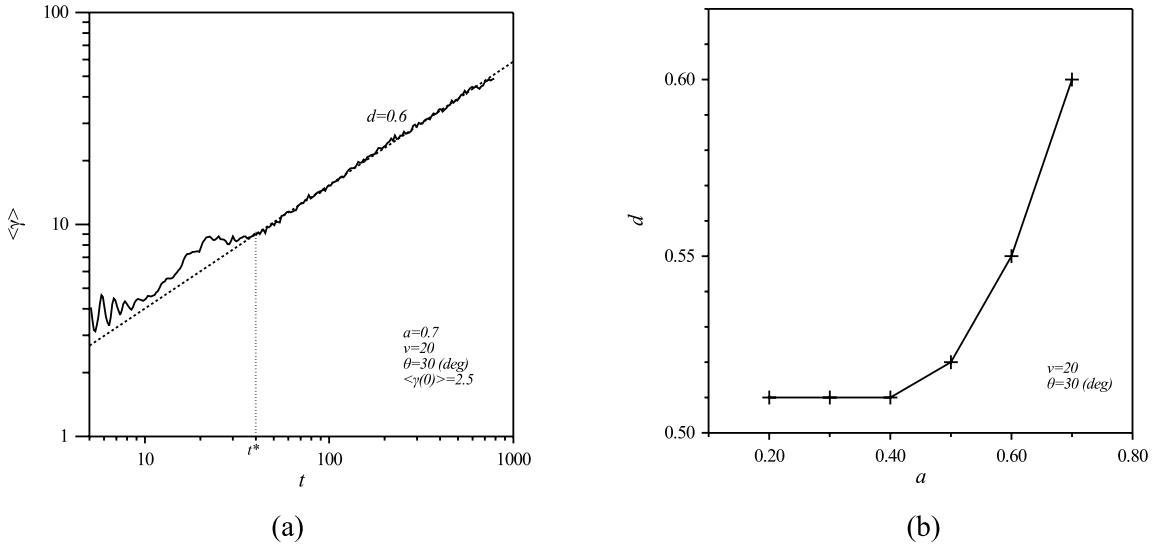

FIG. 6.—(*a*) Plot of the mean energy diffusion in time. We observe that $\log(\langle\gamma\rangle)$ is linearly related to $\log(t)$ for $t > t^*$. The slope d for $\alpha = 0.7$ is $d \sim 0.6$. (*b*) The slope d plotted as a function of the GW amplitude.

central engine a turbulent magnetic field will be formed. Inside this complex magnetic topology, a distribution of three-dimensional magnetic neutral sheets (magnetic null surfaces) with characteristic length l will be developed (see Fig. 7 and the relevant studies on the solar atmosphere [Bulanov & Sakai 1997; Albright 1999; Longcope & Klapper 2002; Longcope, Brown, & Priest 2003]). These three-dimensional surfaces naturally appear and disappear inside driven MHD turbulent plasmas and are randomly distributed inside the atmosphere of the central engine. It is well known that the neutral sheets will act as localized dissipation regions and will accelerate particles (Nodes et al. 2003). The turbulent atmosphere of the central engine will sporadically emit weak X-ray and possibly γ-ray bursts for relatively long times before the collapse of the massive magnetized star and subsequent formation of a black hole or the merging of neutron star binaries. We suggest that numerous weak bursts are present and remain unobserved.

In this article we emphasize the role of the GW passing through magnetic neutral sheets and claim that the GW will enhance dramatically the acceleration process inside the neutral sheet, causing very intense bursts. According to the arguments presented in §§ 2 and 3, the GW can resonate with the electrons only when the magnetic field is weak (in the vicinity of the magnetic null surface). Inside the neutral sheet the synchrotron emission losses are negligible, so the acceleration is very efficient. Electrons escaping from the neutral sheet to the super-strong magnetic field, expected in the atmosphere of the central engine, transfer very efficiently their energy that is perpendicular to the magnetic field to synchrotron radiation, creating spiky localized bursts. The relativistic electrons retain the energy that is parallel to the magnetic field and travel along the field lines until they reach the dense ambient plasma and deposit their energy via collisions, causing other types of longer lived bursts (e.g., X-ray and optical flashes; see Fig. 8*a*).

We suggest thus that the creation of a network of localized accelerators with characteristic length $l_{\rm acc}$ that are spread in relatively large volumes inside the turbulent atmosphere of the central engine will be responsible for the bursty emission. The amplitude of the GW decays as it propagates away from the central engine as $\alpha \sim 1/r$. When $\alpha \ll a_c$ and/or the magnetic topology does not allow formation of magnetic neutral sheets, the GW stops to interact with electrons, and this indicates the end of the burst. So the overall duration of the burst is approximately $\Delta T \sim \Delta L/c$, where ΔL is the length of the characteristic layer where the interaction of the GW with the particles is efficient (see Fig. 8*b*).

4.1. *Energy Spectrum*

Let us now discuss another very important observational fact. It is well documented that the observed spectrum of the synchrotron radiation has a power-law shape. This implies that the energy distribution causing the synchrotron radiation has also a power-law dependence in energy:

$$N(\gamma) \sim \gamma^{-\epsilon},$$

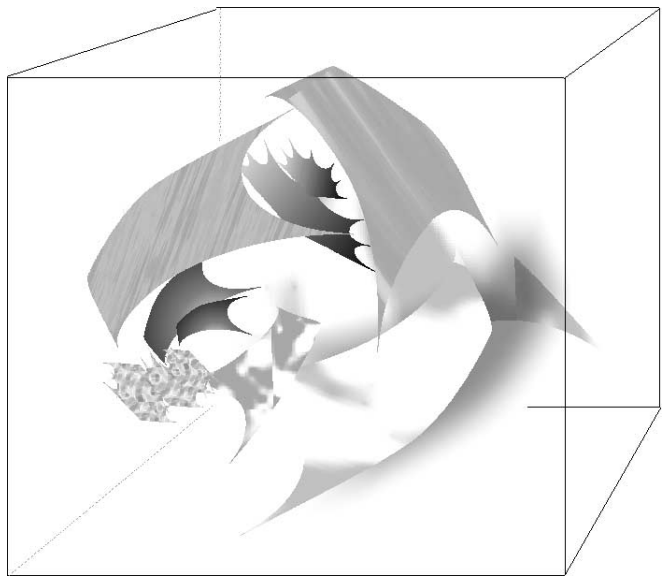

FIG. 7.—Schematic representation of the thin three-dimensional magnetic null sheets that appear spontaneously and densely fill a driven turbulent magnetized plasma.

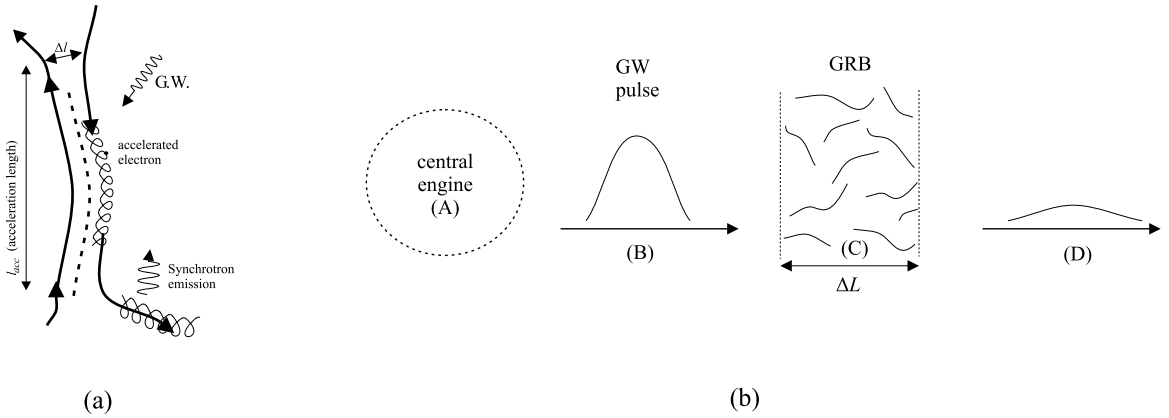

FIG. 8.—(*a*) Propagation of a GW through a magnetic neutral sheet accelerates electrons very efficiently. Relativistic electrons stream away from the accelerator and emit a pulse of synchrotron radiation when they reach the superstrong magnetic fields. The dashed line represents the magnetic field null surface, and $l_{\rm acc}$ is the acceleration length. (*b*) A collection of magnetic neutral sheets is formed inside the turbulent atmosphere (region C) of the central engine (region A). A GW pulse propagating away from the central engine and passing through region C will form numerous γ-ray spikes by accelerating particles near the magnetic null surfaces. The superposition of these spikes forms a short-lived burst. The total burst duration is approximately 100 s ($\Delta T \sim \Delta L/c$), but it is composed of many short spikes lasting less than a second (l/c). The GW pulse will become very weak and the density of the magnetic null surfaces will drop dramatically in region D, and this will mark the end of the burst.

where $\epsilon \simeq 1.8-2.0$ (e.g., see Schaefer et al. 1994 for γ-ray bursts). These types of energy distribution are usually attributed to a shock wave (or a series of shock waves). The formation of a series of localized shock waves along the streaming plasma injected from the central engine is considered the "standard" model for γ-ray bursts (Piran 1999; Mészáros 2002) and may be of interest in many other astrophysical sources.

The spontaneous formation of magnetic neutral sheets in the three-dimensional turbulent atmosphere of the central engine is not easy to describe. A number of studies on the statistical properties of the magnetic neutral sheets have appeared for the active region of the Sun (Georgoulis, Velli, & Einaudi 1998; Longcope & Noonan 2000; Isliker, Anastasiadis, & Vlahos 2000, 2001; Wheatland 2002; Craig & Wheatland 2002). All these studies are based on the observational fact that flares follow a specific distribution in energy (Crosby, Aschwanden, & Dennis 1993).

An important concept from the study of three-dimensional MHD turbulence is that a hierarchy of magnetic neutral sheets formed, with a distribution of characteristic lengths given by the function

$$N(l) \sim l^{-b}. \tag{17}$$

This scaling follows the energy distribution of flares, and the most probable value for b is $3/2$. In other words, inside a turbulent magnetized plasma, a large number of magnetic neutral surfaces with small characteristic lengths, and very few large-scale magnetic neutral sheets, will be present. The exponent for the solar atmosphere, according to the studies reported earlier, is roughly equal to $b \sim 1-2$ and is related to the statistics of X-ray bursts (Crosby et al. 1993). The GW will accelerate electrons only in the brief period when it passes through the magnetic neutral sheet, so the acceleration time will also follow a similar scaling law since

$$t_{\rm acc} \sim l_{\rm acc}/c. \tag{18}$$

We have shown in Figure 6 that the mean energy of the accelerated particles increases with time according to a simple power law as well. Combining equations (17) and (18), we derive first the distribution of t, which is a function of l. We have $N(t)\,dt = N(l)\,dl$, or $N(t) = N(l)(dl/dt)$, which yields, when neglecting the constants,

$$N(t) \sim t^{-b}. \tag{19}$$

We determine next the distribution of γ (or, more precisely, of $\langle\gamma\rangle$), which is a function of t. We start again from the relation $N(\gamma)\,d\gamma = N(t)\,dt$, or $N(\gamma) = N(t)(dt/d\gamma)$. We insert equation (19), $N(\gamma) = t^{-b}(dt/d\gamma)$, and we replace t on the right-hand side using equation (16),

$$N(\gamma) = (\gamma^{1/d})^{-b}\,\frac{d(\gamma^{1/d})}{d\gamma}$$

or, on taking the derivative and rearranging,

$$N(\gamma) = \gamma^{(-b+1-d)/d}. \tag{20}$$

Using typical values of $d \sim 0.5$ (see Fig. 6) and $b \sim 3/2$, we estimate the exponent of the energy distribution to be around 2.

4.2. *Energetics*

The energy transferred from the GW to the high-energy particles by passing through one neutral sheet is

$$E_{\rm ns} \sim \left(\frac{n_t}{n_0}\right) n_0 (l_{\rm acc}^2 \Delta l)\gamma mc^2, \tag{21}$$

where n_0 is the electrons' density, n_t are the electrons at the tail of the local Maxwellian, and Δl is the thickness of the magnetic neutral sheet. The filling factor of neutral sheets inside the atmosphere of the central engine is assumed to be f. So the total number of magnetic neutral sheets expected to interact with the GW is $(\Delta L)^3 f/l^2\Delta l$, and the total energy transferred to the plasma

$$W_{\rm tot} \sim \left[f\,\frac{(\Delta L)^3}{l^2\Delta l}\right]\left[\frac{n_t}{n_0} n_0\left(l_{\rm acc}^2\Delta l\right)\gamma mc^2\right]. \tag{22}$$

Using typical numbers $n_0 = 10^{12}$ cm^{-3}, $n_t/n_0 \sim 10^{-1}$, $\gamma = 100$, $l_{\rm acc} \sim 10^8$ cm, $\Delta l \sim 10^7$ cm, and $f \sim 10^{-1}$ and assuming

that the burst duration is 1 s, which implies that $\Delta L \sim 3 \times 10^{12}$ cm, the total energy estimated is approximately 10^{47}–10^{48} ergs. The total burst duration is around 100 s, but the burst is composed of many short bursts lasting less than a second (l/c).

We can now list several characteristics of the bursty emission driven by the model proposed above:

1. A fraction of the energy carried by the orbital energy of the neutron stars at merger will go to the GW, and a portion of this energy will be transferred to the high-energy electrons.
2. The topology of the magnetic field varies from event to event, so every burst has its own characteristics.
3. The superposition of many small-scale localized sources produces a fine time structure on the burst.
4. The superposition of null surfaces with a power-law distribution of the acceleration lengths will result in a power-law energy distribution for the accelerated electrons and an associated synchrotron radiation emitted by the relativistic electrons.
5. The decay of the amplitude of the GW and/or the lack of magnetic neutral sheets away from the central engine will mark the end of the burst but not necessarily the end of other types of bursts, since the cooling of the ambient turbulent plasma has a much longer timescale.

It is worth drawing an analogy between the elements used to build our model for this bursty emission and two significant developments in studies of solar flares and the Earth's magnetic tail. (1) Galsgaard & Nordlund (1997) studied the dynamic formation of current sheets (current sheets are not always associated with neutral sheets) in the solar atmosphere. They found that the irregular motion of the magnetic footpoints, caused by the turbulent convection zone, forces the magnetic topologies to form a hierarchy of three-dimensional current sheets inside the complex magnetic topologies above active regions. (2) Ambrosiano et al. (1988) studied the passage of low-frequency waves (Alfvén waves) through a two-dimensional neutral sheet. They discovered that the acceleration of charged particles is greatly enhanced by the presence of the Alfvén waves.

We believe that solar flares, the Earth's magnetotail, and the GW-driven bursts share two important characteristics, namely, the formation of three-dimensional magnetic null surfaces coupled with the passage of waves through these surfaces (Alfvén waves for the Sun and the Earth's magnetotail and GWs for the bursts analyzed in this article), although the external drivers and the energetics of the bursts produced are clearly very different.

5. SUMMARY

In this article we have studied an efficient mechanism for transferring the energy released from a central engine to the turbulent plasma in its atmosphere. We have analyzed the nonlinear interaction of a GW with electrons. We have shown that electrons in the tail of the ambient plasma are accelerated efficiently, reaching energies of up to hundreds of MeV in less than a second, when (1) the amplitude of the GW is above a typical value 0.005–0.5 and (2) the magnetic field is relatively weak, $B_0 \sim 10^{-4}$ G, for a GW with a typical frequency 1–10 KHz.

On the basis of these findings, we propose that pulsed GWs emitted from the central engine will interact with the ambient plasma in the vicinity of the magnetic neutral sheets formed naturally inside externally driven turbulent MHD plasmas. Magnetic neutral sheets have characteristic lengths $l \sim 10^7$ – 10^8 cm and are short-lived three-dimensional surfaces. Although these structures are efficient accelerators, we are emphasizing in this article only the role of the GW passing through these surfaces, since we focus our attention on the very strong and bursty sources. The GW passing through the neutral sheets will accelerate electrons to very high energies. Relativistic electrons escape from the magnetic neutral sheets, radiating synchrotron emission as soon as they reach the very strong magnetic fields.

We have studied the collective emission of thousands of short-lived (less than a second) synchrotron pulses, created during the passage of the GW through a relatively large volume. The relativistic electrons losing most of their energy that is perpendicular to the magnetic field to synchrotron radiation retain the parallel energy and heat the ambient plasma, emitting other types of longer lived bursts, e.g., X-rays and optical flushes.

We have also shown that if the acceleration length follows a simple scaling law [$N(l_{\rm acc}) \sim l_{\rm acc}^{-b}$] and that if, as shown, $\langle\gamma\rangle \sim t_{\rm acc}^{\,d}$, the energy distribution also follows a power-law scaling [$N(\langle\gamma\rangle) \sim \langle\gamma\rangle^{(-b+1-d)/d}$], which for reasonable values of $b \sim 3/2$ and $d \sim 1/2$ agrees remarkably well with the energy distributions inferred from the observations.

We are suggesting that numerous bursts are still present before and after the passage of the GW since the magnetic neutral sheet acts as an efficient particle accelerator. The GW passage simply enhances the acceleration process and makes many short-lived spikes become visible. We propose that a more thorough analysis of the statistical properties of the bursty emission, with the main emphasis on the low-energy part of the frequency distribution, will give important insight on the processes mentioned here.

A detailed model of the interaction of a GW with turbulent MHD plasma is currently under study, and we hope to develop an even more efficient energy transfer from the GW to the plasma by, e.g., triggering the interaction (percolation) of many null sheets during the passage of the GW. We hope that this will lead us to an alternative scenario for the still unresolved questions related to the acceleration mechanism in the atmosphere of the central engines and the physical processes behind the X-ray and γ-ray bursts.

We thank Heinz Isliker and the anonymous referees for many helpful suggestions that improved our article substantially.

REFERENCES

Albright, B. J. 1999, Phys. Plasmas, 6, 4222
Ambrosiano, J., Matthaeus, W., Goldstein, M. L., & Plante, D. 1988, J. Geophys. Res., 93, 14383
Arnol'd, V. I, Kozlov, V. V., & Neishtadt, A. I. 1987, in Dynamical Systems III, ed. V. I. Arnol'd (Berlin: Springer), 116
Baumgarte, T. W., & Shapiro, S. L. 2003, ApJ, 585, 930
Brodin, G., & Marklund, M. 1999, Phys. Rev. Lett., 82, 3012
Brodin, G., Marklund, M., & Dunsby, P. K. S. 2000, Phys. Rev. D, 62, 104008
Brodin, G., Marklund, M., & Servin, M. 2001, Phys. Rev. D, 63, 124003
Bulanov, S. V., & Sakai, J.-I. 1997, J. Phys. Soc. Japan, 66, 3477
Chirikov, B. V. 1979, Phys. Rep., 52, 264
Cooperstock, F. I. 1968, Ann. Phys., 47, 173
Craig, I. J. D., & Wheatland, M. 2002, Sol. Phys., 211, 275
Crosby, N. B., Aschwanden, N. J., & Dennis, B. R. 1993, Sol. Phys., 143, 275

Daniel, J., & Tajima, T. 1997, Phys. Rev. D, 55, 5193
Demianski, M. 1985, Relativistic Astrophysics (Oxford: Pergamon)
Denisov, V. I. 1978, Soviet Phys.–JETP, 42, 209
DeWitt, B. S., & Breheme, R. W. 1960, Ann. Phys., 9, 220
Dimmelmeier, H., Font, A. J., & Muller, E. 2002, A&A, 393, 523
Fryer, C. L., Holz, D. E., & Hughes, S. T. 2002, ApJ, 565, 430
Galsgaard, K., & Nordlund, A. 1997, J. Geophys. Res., 102, 231
Georgoulis, M. K., Velli, M., & Einaudi, G. 1998, ApJ, 497, 957
Gerlach, U. H. 1974, Phys. Rev. Lett., 32, 1023
Grishchuk, L. P., & Polnarev, A. G. 1980, in General Relativity and Gravitation: One Hundred Years after the Birth of Einstein, Vol. 2, ed. A. Held (New York: Plenum Press), 393
Isliker, H., Anastasiadis, A., & Vlahos, L. 2000, A&A, 363, 1134
———. 2001, A&A, 377, 1068
Kleidis, K., Varvoglis, H., & Papadopoulos, D. 1993, A&A, 275, 309
Kleidis, K., Varvoglis, H., Papadopoulos, D., & Esposito, F. P. 1995, A&A, 294, 313
Longcope, D. W., Brown, D. S., & Priest, E. R. 2003, Phys. Plasmas, 10, 3321
Longcope, D. W., & Klapper, I. 2002, ApJ, 579, 468
Longcope, D. W., & Noonan, E. J. 2000, ApJ, 542, 1088
Macdonald, D., & Thorne, K. S. 1982, MNRAS, 198, 345
Macedo, P. G., & Nelson, A. G. 1982, Phys. Rev. D., 28, 2382
Marklund, M., Brodin, G., & Dunsby, P. K. S. 2000, ApJ, 536, 875
Mészáros, P. 2002, ARA&A, 40, 137
Misner, C. W., Thorne, K. S., & Wheeler, J. A. 1973, Gravitation (San Francisco: Freeman)
Moortgat, J., & Kuijpers, J. 2003, A&A, 402, 905
Nodes, C., Birk, G. T., Lesch, H., & Schopper, R. 2003, Plasma Phys., 10, 835
Ohanian, H. C. 1976, Gravitation and Spacetime (New York: Norton)
Papadopoulos, D., & Esposito, F. 1981, ApJ, 248, 783
Papadopoulos, D., Stergioulas, N., Vlahos, L., & Kuijpers, J. 2001, A&A, 377, 701
Piran, T. 1999, Phys. Rep., 314, 575
Ruffert, M., & Janka, H. T. 1998, A&A, 338, 535
Sagdeev, R. Z., Usikov, D. A., & Zaslavsky, G. M. 1988, Nonlinear Physics (New York: Harwood)
Schaefer, B. E., et al. 1994, in AIP Conf. Proc. 307, Gamma-Ray Bursts: Second Workshop, ed. G. J. Fishman, J. J. Brainerd, & K. Hurley (New York: AIP), 271
Servin, M., Brodin, G., Bradley, M., & Marklund, M. 2000, Phys. Rev. E, 62, 8493
Servin, M., Brodin, G., & Marklund, M. 2001, Phys. Rev. D, 64, 024013
Shibata, M., & Uryu, K. 2002, Prog. Theor. Phys., 107, 265
Varvoglis, H., & Papadopoulos, D. 1992, A&A, 261, 664
Wheatland, M. 2002, Sol. Phys., 208, 33
Zel'dovich, Y. B. 1974, Soviet Phys.–JETP, 38, 652